The Intrinsic Electrostatic Potential and the Intermediate Ring of Charge in the Acetylcholine Receptor Channel

Gary G. Wilson,* Juan M. Pascual,*‡ Natasja Brooijmans,* Diana Murray,§ and Arthur Karlin*‡§‖

From the *Center for Molecular Recognition, ‡Department of Neurology, §Department of Biochemistry and Molecular Biophysics, and ‖Department of Physiology and Cellular Biophysics, College of Physicians and Surgeons, Columbia University, New York, New York 10032

abstract A ring of aligned glutamate residues named the intermediate ring of charge surrounds the intracellular end of the acetylcholine receptor channel and dominates cation conduction (Imoto et al., 1988). Four of the five subunits in mouse-muscle acetylcholine receptor contribute a glutamate to the ring. These glutamates were mutated to glutamine or lysine, and combinations of mutant and native subunits, yielding net ring charges of -1 to -4, were expressed in *Xenopus laevis* oocytes. In all complexes, the α subunit contained a Cys substituted for αThr244, three residues away from the ring glutamate αGlu241. The rate constants for the reactions of αThr244Cys with the neutral 2-hydroxyethyl-methanethiosulfonate, the positively charged 2-ammonioethyl-methanethiosulfonate, and the doubly positively charged 2-ammonioethyl-2'-ammonioethanethiosulfonate were determined from the rates of irreversible inhibition of the responses to acetylcholine. The reagents were added in the presence and absence of acetylcholine and at various transmembrane potentials, and the rate constants were extrapolated to zero transmembrane potential. The intrinsic electrostatic potential in the channel in the vicinity of the ring of charge was estimated from the ratios of the rate constants of differently charged reagents. In the acetylcholine-induced open state, this potential was -230 mV with four glutamates in the ring and increased linearly towards 0 mV by $+57$ mV for each negative charge removed from the ring. Thus, the intrinsic electrostatic potential in the narrow, intracellular end of the open channel is almost entirely due to the intermediate ring of charge and is strongly correlated with alkali-metal-ion conductance through the channel. The intrinsic electrostatic potential in the closed state of the channel was more positive than in the open state at all values of the ring charge. These electrostatic properties were simulated by theoretical calculations based on a simplified model of the channel.

key words: nicotinic • mutagenesis • reaction kinetics • conductance • selectivity

INTRODUCTION

Lipid bilayers are almost impermeable to inorganic ions because the energy of a monovalent ion in lipid is 40 kcal/mol higher than in water (Parsegian, 1969). Ion channels overcome this barrier and conduct ions across the bilayer both rapidly and selectively. There are still electrostatic barriers to ion permeation because the water-filled lumen of an ion channel is surrounded by protein and lipid characterized by low dielectric constants, and, in selective channels, ions pass the narrow selectivity filter partially dehydrated (Hille, 1992). These barriers, however, are lowered by interactions of the permeating ion with charged residues and with side-chain and backbone dipoles (Green and Andersen, 1991; Green and Lu, 1995; Syganow and von Kitzing, 1995; Eisenberg, 1996).

Electrostatic interactions have been described in a number of channels. The gramicidin A channel, a most efficient conductor of alkali-metal ions, has no charged residues, but interactions with backbone carbonyl dipoles and with oriented waters stabilize monovalent cations in the channel (Andersen and Koeppe, 1992; Roux and Karplus, 1994). In a bacterial K^+ channel, a high-resolution structure shows that one site of K^+ occupation is stabilized by the dipole moments of four symmetrically oriented α-helices, and occupation of two selectivity-determining sites is stabilized by backbone carbonyls (Doyle et al., 1998; Roux and MacKinnon, 1999). Selectivity in Ca^{2+} channels (Yang et al., 1993) and in CFTR (Guinamard and Akabas, 1999) depends on charged residues facing the lumen. Charged residues at the ends of the acetylcholine (ACh)[1] receptor channel lumen play crucial roles in conductance and selectivity (Imoto et al., 1988; Konno et al., 1991; Corringer et al., 1999), and lumen-facing polar side chains (Leonard et al., 1988; Cohen et al., 1992; Villarroel et al., 1992) and backbone peptide bonds (Corringer et al., 1999) also affect conductance and selectivity.

Address correspondence to Dr. Arthur Karlin, Center for Molecular Recognition, Columbia University, 630 West 168th Street, New York, NY 10032. Fax: 212-305-5594; E-mail: ak12@columbia.edu

[1]*Abbreviations used in this paper:* ACh, acetylcholine; AEAETS, 2-ammonioethyl-2'-ammonioethanethiosulfonate dichloride; MTSEA, 2-ammonioethyl-methanethiosulfonate bromide; MTSEH, 2-hydroxyethyl-methanethiosulfonate.

Electrostatic-potential profiles in the lumen of the ACh receptor channel have been determined experimentally (Pascual and Karlin, 1998) and calculated theoretically (Adcock et al., 1998). Although the two profiles differ in detail, they each contain a cation-stabilizing well of negative electrostatic potential.

The ACh receptor is a complex of five subunits, two α and one each of β, γ (or ϵ), and δ, which surround the central channel (see Fig. 1 A) (Karlin and Akabas, 1995; Hucho et al., 1996; Corringer et al., 2000). The subunits share a common membrane topology (see Fig. 1 B), and the membrane-spanning portion of the channel is lined by residues in the M2 membrane-spanning segments, and to a lesser extent by residues in the M1 membrane-spanning segments (Zhang and Karlin, 1998).

The intrinsic electrostatic potential in the channel due to fixed and induced charges in the receptor (at zero transmembrane potential) was determined at three positions along the αM2 segment, near its cytoplasmic end at αT244, near its middle at αL251, and near its extracellular end at αL258 (Pascual and Karlin, 1998). The intrinsic electrostatic potential ranged from approximately -200 mV in the vicinity of αT244 to -25 mV at αL258. The determination was based on a comparison of the rate constants for the reactions of differently charged, but otherwise similar, organic reagents with Cys substituted by site-directed mutagenesis for residues facing the channel lumen. The reactions were monitored by their effects on receptor function. The reagents were derivatives of sulfhydryl-specific thiosulfonates (Stauffer and Karlin, 1994), which have been widely used to probe the properties of binding sites and conduction pathways in ion channels and transport proteins (reviewed in Karlin and Akabas, 1998).

The residue αT244, and the aligned residues in the other subunits, are in a narrow region of the channel lumen that constitutes the selectivity filter (Konno et al., 1991; Cohen et al., 1992; Villarroel et al., 1992). This narrow region extends from αG240 to αT244 (see Fig. 1 C) and includes the activation gate (Wilson and Karlin, 1998).[2] This region also includes four aligned Glu, two αE241, one βE252, and one δE255 (see Fig. 1 C). These Glu constitute what Imoto et al. (1988) named the intermediate ring of charge. They found that the potassium conductance of the open ACh receptor channel decreased approximately linearly as they decreased the total negative charge in this ring by mutation: the cation conductance of mutants with a ring charge of -2 was $\sim$20% of the conductance of the wild-type receptor with a ring charge of -4. Also, mutation to Gln of the

five Glu in the intermediate ring of the neuronal $(\alpha 7)_5$ ACh receptor reduced its cation conductance drastically and was a necessary but not sufficient alteration to switch the charge selectivity of this channel from cationic to anionic (Corringer et al., 1999).

We now show that the intrinsic electrostatic potential in the vicinity of αT244 in the open channel is almost entirely due to the intermediate ring of charge. The magnitude of the negative potential decreases linearly as the negative ring charge is decreased, extrapolating to zero potential at a total ring charge of zero. Thus, the negative intrinsic electrostatic potential in the vicinity of the selectivity filter correlates with the cation conductance.

MATERIALS AND METHODS

Mutagenesis and Oocyte Expression

Site-directed mutations were generated in mouse muscle αT244C, wild-type β, and wild-type δ by PCR with *pfu* DNA polymerase (Stratagene Inc.). The PCR product was ligated into the pSP64 vector using appropriate restriction sites, and the cassette was sequenced to confirm the mutation. Mutants were named as <subunit> <wild-type residue> <residue number> <mutant residue>, using single-letter codes for amino acid residues. Capped cRNA was produced by in-vitro transcription with SP6 polymerase. Defolliculated *Xenopus laevis* oocytes were prepared and injected with 50 nl cRNA (100–500 ng/μl) at a ratio of 2α:1β:1γ:1δ, as previously described (Akabas et al., 1992). Injected oocytes were incubated at 18°C in culture medium and used for current recordings after 1–12 d.

Electrophysiology

Currents were recorded under two-electrode voltage-clamp from oocytes in a bath solution containing (mM): 115 NaCl, 2.5 KCl, 1.8 MgCl$_2$, and 10 HEPES, pH 7.2. Oocytes were perfused with bath solution maintained at a temperature of 18°C, at a rate of 7 ml/min. Voltage-recording and current-passing glass electrodes (filled with 3 M KCl) varied in resistance between 0.5 and 1 MΩ. The reference electrode was connected to the bath via an agar bridge. All reagents were applied via the bath. Peak ACh-induced current was measured during a 10-s application of ACh at a concentration $4\times$ EC$_{50}$ for each mutant. There was no evidence of slow desensitization during these 10-s applications. ACh was applied two or three times to each oocyte, and only if the peak currents varied by <5% was the oocyte used further.

The response of mutant receptors to ACh was characterized by fitting the Hill equation to the currents evoked by at least five different ACh concentrations:

$$I = I_{Max}/\{1 + (EC_{50}/[ACh])^n\}, \tag{1}$$

where I_{MAX} is the asymptotic maximum current, EC$_{50}$ is the concentration of ACh evoking half-maximal current, and n is the Hill coefficient.

Reagents

2-Ammonioethyl-methanethiosulfonate bromide [CH$_3$SO$_2$SCH$_2$CH$_2$NH$_3^+$ Br$^-$] (MTSEA) was purchased from Toronto Research Chemicals. 2-Hydroxyethyl-methanethiosulfonate [CH$_3$SO$_2$SCH$_2$

---

[2]Although the accessibilities of these residues from the two sides of the membrane in the open and closed states of the channel are known (Wilson and Karlin, 1998), their distances from the cytoplasmic face of the phospholipid bilayer are not known (see Miyazawa et al., 1999).

CH2OH] (MTSEH) and 2-ammonioethyl-2′-ammonioethanethiosulfonate dichloride [$H_3N^+CH_2CH_2SO_2SCH_2CH_2NH_3^+$ Cl^-_2] (AEAETS) were synthesized as previously described (Pascual and Karlin, 1998). Concentrated stocks were made daily in distilled water and kept in ice until diluted in bath solution just before use (Karlin and Akabas, 1998).

Reaction Rates

As previously described (Pascual and Karlin, 1998), peak current was measured during a 10-s application of ACh followed by a 3-min wash; thiosulfonate reagent was applied in either the absence or presence of ACh, followed by a 3-min wash. This process was repeated several times. The peak ACh-evoked currents were plotted against the cumulative times of exposure to thiosulfonate reagent preceding the responses. Concentrations of thiosulfonate reagent varied from 1 μM to 20 mM for MTSEA, 10 to 20 mM for MTSEH, and 100 nM to 10 mM for AEAETS. The duration of each application of reagent varied from 2 to 120 s in the absence of ACh and from 2 to 20 s in the presence of ACh. Application of ACh alone for these times did not result in slow desensitization. The pseudo-first-order kinetic data were fitted by Eq. 2:

$$I_t = I_\infty + (I_0 - I_\infty)\exp(-k^* t),\qquad(2)$$

where I_t is the peak ACh-evoked current after t seconds of cumulative exposure to thiosulfonate reagent, I_0 is the initial current, I_∞ is the peak current when the reaction is complete, and k^* is the pseudo-first-order rate constant. The second-order rate constant, κ, is given by Eq. 3:

$$\kappa = k^*/[\text{thiosulfonate}].\qquad(3)$$

To determine the rate constant for the reaction at zero transmembrane potential, either we extrapolated the rate constants for the reaction at three non-zero membrane potentials to zero membrane potential, or we measured the reaction rate at 0 mV directly. Whatever the holding potential was during the application of the reagent, the holding potential was always −50 mV during the test responses to ACh.

Intrinsic Electrostatic Potential

We determined the rate constants, κ, for the reactions of MTSEA, MTSEH, and AEAETS with αT244C at zero transmembrane potential. We previously determined the rate constants, k_{ME}, for the reactions of these reagents with 2-mercaptoethanol [$HSCH_2CH_2OH$] in bulk solution (Pascual and Karlin, 1998). We formed a ratio of ratios, ρ_0, of the rate constants for pairs of the thiosulfonate reagents (at zero transmembrane potential), as follows:

$$\rho_0 = ({}^1\kappa/{}^2\kappa)/({}^1k_{ME}/{}^2k_{ME}),\qquad(4)$$

where ${}^1\kappa$ is the second-order rate constant for the reaction of either MTSEA or AEAETS with the Cys in αT244C and ${}^2\kappa$ is in each case the second-order rate constant for the reaction of MTSEH with αT244C. ${}^1k_{ME}$ is the second-order rate constant for the reaction of either MTSEA or AEAETS with 2-mercaptoethanol in solution, and ${}^2k_{ME}$ is the second-order rate constant for the reaction of MTSEH with 2-mercaptoethanol in solution. Under conditions of quasi-equilibrium and low saturation of the reaction site with the reagent:

$$\rho_0 \cong \exp(-\Delta\Delta G^0/RT),\qquad(5)$$

where $\Delta\Delta G^0 = \Delta G^0_1 - \Delta G^0_2$, the difference in the standard free energies of association of reagent 1 and reagent 2 with the reaction site. The standard free energy of association of the first reagent, $\Delta G^0_1 = G^0_{S,1} - G^0_{EX,1} - G^0_S$, where $G^0_{S,1}$ is the standard free energy of the complex of the site and reagent 1, $G^0_{EX,1}$ is the standard free energy of the reagent 1 in the extracellular solution, and G^0_S is the standard free energy of the unoccupied site. Similarly, $\Delta G^0_2 = G^0_{S,2} - G^0_{EX,2} - G^0_S$. The terms G^0_S cancel in $\Delta\Delta G^0$.

For two reagents that are similar in all respects except charge, we assume that all contributions to $\Delta\Delta G^0$ cancel, except the difference in electrostatic free energies of association for the two reagents that depend on reagent charge. We equate this difference in electrostatic free energies and, hence, $\Delta\Delta G^0$ to $(z_1 - z_2)F\psi_S$, where z_1 is the charge of MTSEA (+1) or AEAETS (+2), z_2 is the charge of MTSEH (0), and ψ_S is the intrinsic electrostatic potential in the channel close to the charge on the reagent when it is reacting with the Cys substituted for αT244. Therefore, as derived previously (Pascual and Karlin, 1998):

$$\rho_0 \cong \exp[-(z_1 - z_2)(F/RT)\psi_S].\qquad(6)$$

Theoretical Calculation of the Standard Free Energy of Association

In the absence of a high-resolution structure for the receptor, we modeled the channel lumen as a water-filled cylinder embedded in a uniform, low-dielectric slab, representing both the membrane-spanning domain of the receptor and the phospholipid bilayer (see Fig. 8). The electrostatic standard free energy, ΔG^0, of transfer (or association) of a reagent molecule or a Na^+ from bulk solution to a given location within the model channel was defined as ΔG^0_1 above and calculated as the electrostatic energy of the complex of the reagent or inorganic ion at a given position in the channel, minus the self-energy of the reagent or ion in bulk solution, and minus the electrostatic energy of the unoccupied channel with its charges (Sharp and Honig, 1990). The electrostatic energies were calculated from a numerical solution of the nonlinear Poisson-Boltzmann equation (Gilson et al., 1987). The calculations were performed with a grid box 37.7 Å per side, divided into 113 × 113 × 113 cells at a scale of three grids per angstrom.

We built molecular models of the reagents MTSEA, MTSEH, and AEAETS with the Biopolymer module of the program InsightII (Molecular Simulations Inc.). The models were optimized using MOPAC in the MOPAC/AMPAC module of InsightII. Subsequently, the structures were energy-minimized with the program CHARMM (Brooks et al., 1983) using the CHARMM22 parameters and force field (Mackerell et al., 1992). Atomic charges and radii were taken from the PARSE parameter set (Sitkoff et al., 1994). For the calculations presented, the molecular models were placed on the axis of the channel with the ammonium group or the hydroxyl group in the plane of the Glu ring and the ether sulfur juxtaposed to the position of the substituted Cys in αT244C. We used these models to include the effects of size and charge distribution on the electrostatic interactions of the reagents with the channel. In the case of Na^+, the Born radius of 1.68 Å was used (Rashin and Honig, 1985), and the ion was placed at several positions along the axis.

Because anions cannot penetrate the cation-selective ACh channel to the vicinity of αT244 (Akabas et al., 1994), we calculated the electrostatic free energy with zero ionic strength in the channel. Because ionic strength has only a small effect on the self-energy of the charged reagents and of Na^+ in bulk solution, we also set the ionic strength in the bulk solution to zero.

Expression of Glutamate-ring Mutants

The aligned residues αE241, βE252, and δE255 (Fig. 1 C) were mutated to alter the ring charge. We designate the subunits with a superscript to indicate the charge of the residue at the ring position. The wild-type subunits are designated α^-, β^-, γ^0, and δ^-. The mutant αE241Q is designated α^0, βE252Q is designated β^0, βE252K is designated β^+, and δE255Q is designated δ^0. In all cases, α contained the mutation T244C, so that α^- contains the mutation T244C, and α^0 contains both mutations, T244C and E241Q. The complexes tested were: $\alpha^-_2\beta^-\gamma^0\delta^-$ (i.e., the pseudo-wild type receptor with αT244C), $\alpha^-_2\beta^0\gamma^0\delta^-$, $\alpha^-_2\beta^-\gamma^0\delta^0$, $\alpha^0_2\beta^-\gamma^0\delta^-$, $\alpha^-_2\beta^+\gamma^0\delta^-$, $\alpha^0_2\beta^0\gamma^0\delta^-$, and $\alpha^0_2\beta^0\gamma^0\delta^0$. These combinations had -4 to 0 net charges in the glutamate ring.

The responses of each of these complexes to a range of ACh concentrations were fitted by the Hill equation (Eq. 1), which yielded I_{MAX}, EC_{50}, and n. Despite the expected lower single-channel conductance in the mutants with decreased ring charge (Imoto et al., 1988), usable ACh-induced currents were obtainable within 5 d of injection in all cases except that of $\alpha^0_2\beta^0\gamma^0\delta^0$, which never gave more than -50 nA in response to ACh and was not tested further. For the oocytes and mutants used, the mean I_{MAX} varied from approximately -500 to $-2,000$ nA (Fig. 2 A). These whole-cell currents, of course, depend on the extent of expression and the gating and desensitization kinetics as well as on the single-channel conductance. $\alpha^-_2\beta^+\gamma^0\delta^-$ gave unstable currents that often underwent spontaneous runup or rundown of repeated responses, and we could not use it for measuring reaction rates.

With decreasing ring charge, the EC_{50} for ACh increased modestly from 13 μM for the pseudo-wild type to $\sim$50 μM for $\alpha^0_2\beta^0\gamma^0\delta^-$ or 1.6-fold increase in EC_{50} per unit decrease in negative charge (Fig. 2 B). Under the conditions of our experiments, wild-type receptor has an EC_{50} for ACh of $\sim$3 μM (Akabas et al., 1994). Hill coefficients for all mutants ranged from 1.4 to 1.8.

Thiosulfonate Reaction Rates

For each of the mutants, we recorded ACh-induced currents between repeated exposures to thiosulfonate reagents. Typical results are shown for $\alpha^0_2\beta^0\gamma^0\delta^-$ exposed to MTSEA in the absence (Fig. 3 A) and in the presence (Fig. 3 C) of ACh. The peak currents of the ACh-induced test responses declined as a first-order process (Fig. 3, B and D). The exponential fits to these data yielded pseudo-first order rate constants for the reactions of MTSEH, MTSEA, and AEAETS with each of the Glu-ring mutants.

For most mutants and reagents, rate constants were measured at three holding potentials. A typical set of rate constants are shown in Fig. 4 for the reactions of MTSEH, MTSEA, and AEAETS, in the absence and presence of ACh, with $\alpha^0_2\beta^0\gamma^0\delta^-$. Only for AEAETS in the presence of ACh did the rate constant depend significantly on the holding potential, as previously found with $\alpha^-_2\beta^-\gamma^0\delta^-$ (Pascual and Karlin, 1998). For none of these reagents in the absence of ACh did the rate constants depend on the holding potential. For the reactions independent of holding potential, the rate constants at 0 mV were taken as the means of the determinations at the three holding potentials. For the voltage-dependent reaction, the rate constant at 0 mV was estimated by extrapolation (Fig. 4). The reactions MTSEA and AEAETS with $\alpha^-_2\beta^-\gamma^0\delta^0$ were carried out at a holding potential

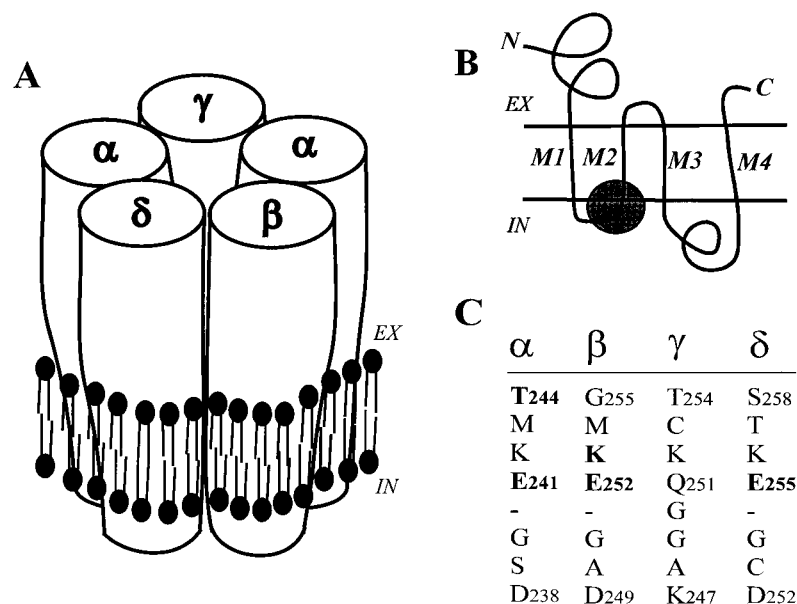| α	β	γ	δ
T244	G255	T254	S258
M	M	C	T
K	**K**	K	K
E241	**E**252	Q251	**E**255
-	-	G	-
G	G	G	G
S	A	A	C
D238	D249	K247	D252

Figure 1. Schematic representation of the muscle-type ACh receptor. (A) The receptor complex in the membrane. (B) The common membrane topology of its subunits. (C) The aligned sequences of four mouse-muscle receptor subunits at the cytoplasmic ends of their M2 membrane-spanning segments and the M1–M2 loops. The sequences in C are from the region of the subunits covered with the shaded circle in B.[2] The residues that were mutated in the work described here are in bold type. The numbering is that of the mature sequences.
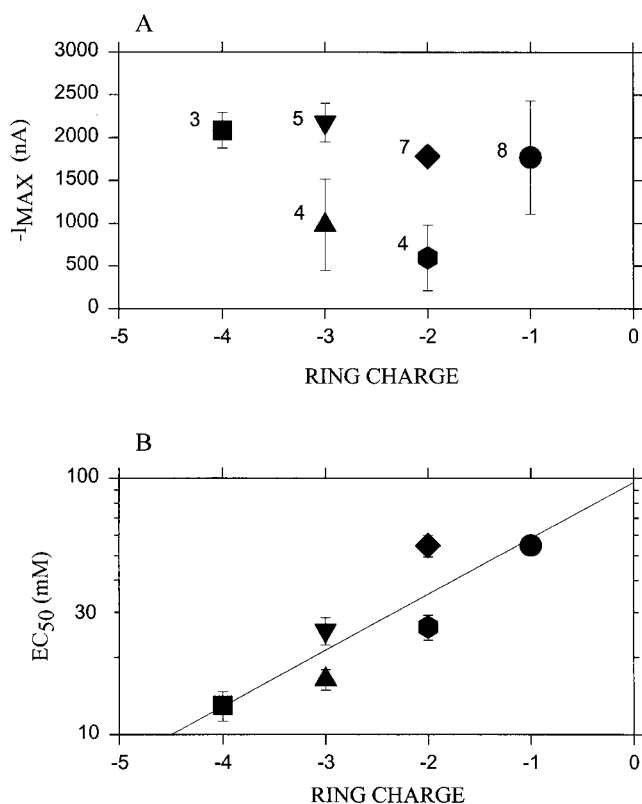
Figure 2. Responses of complexes of subunits mutated in the Glu ring. Oocytes were injected with all four types of subunits. In all cases, α contained the mutation T244C; this is designated α^- if E241 is not also mutated, and α^0 if in addition E241 is mutated to Q (i.e., the superscript indicates the charge of the residue in the position of the Glu ring). Wild-type β is designated β^-; β with the mutation E252 to Q is designated β^0; and β with the mutation E252 to K is designated β^+. Wild-type γ is designated γ^0. Wild-type δ is designated δ^-, and δ with the mutation E255 to Q is designated δ^0. The complexes tested were: $\alpha^-_2\beta^-\gamma^0\delta^-$ (i.e., a pseudo wild type with only αT244 mutated to C; ring charge, -4; square); $\alpha^-_2\beta^0\gamma^0\delta^-$ (ring charge, -3; up triangle); $\alpha^-_2\beta^-\gamma^0\delta^0$ (ring charge, -3; down triangle); $\alpha^0_2\beta^-\gamma^0\delta^-$ (ring charge, -2; diamond); $\alpha^-_2\beta^+\gamma^0\delta^-$ (ring charge, -2; hexagon); and $\alpha^0_2\beta^0\gamma^0\delta^-$ (ring charge, -1; a circle). (A) The average maximum current ($-I_{MAX}$) obtained from the fit of the Hill equation to the responses at various concentrations of ACh. (B) The average EC_{50} obtained from the fit of the Hill equation. The least-squares linear fit to the $\log(EC_{50})$ is shown. In each case, the abscissa is the sum of the charges in the ring. The numbers of independent experiments are indicated next to the symbols. The bars represent the standard errors of the means.

of 0 mV, and thus the rate constants at 0 mV were determined directly.

The rate constants at zero transmembrane potential for each reagent varied with the total charge in the Glu ring (Fig. 5). The log (rate constant) was a linear function of ring charge. The rate constants for MTSEA decreased by a multiplicative factor of 0.6 in the absence and 0.4 in the presence of ACh, per unit decrease of negative charge. The rate constants for AEAETS increased by a factor of 2.0 in the absence of ACh, and decreased
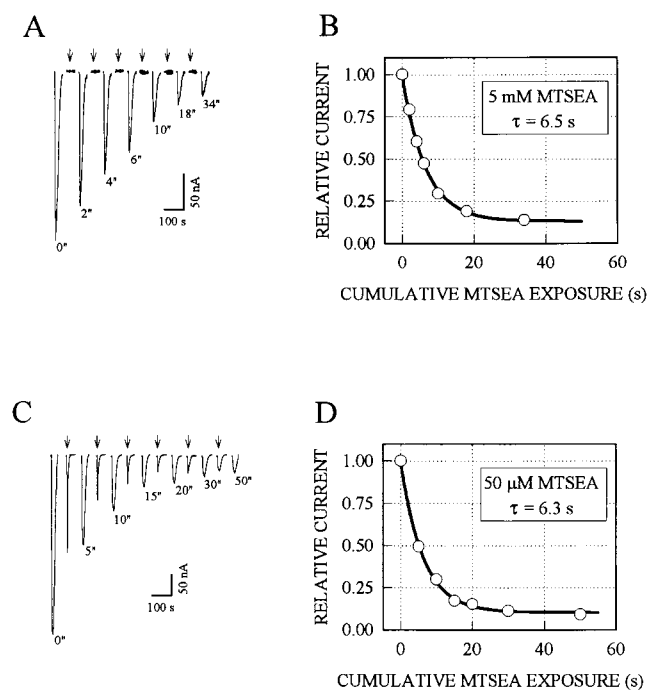

Figure 3. Kinetics of the reaction of MTSEA with the Cys at α244 exemplified with $\alpha^0_2\beta^0\gamma^0\delta^-$. MTSEA was applied to oocytes expressing $\alpha^0_2\beta^0\gamma^0\delta^-$ in both the closed (A and B) and open (C and D) states at a holding potential of -50 mV. The sequence of applications to the oocytes was: 200 μM ACh for 10 s; bath solution for 3 min; 5 mM MTSEA for 2–16 s (beginning at arrows) for the closed state (A) or 50 μM MTSEA together with 200 μM ACh for 5–20 s (arrows) for the open state (C); bath solution for 3 min. This sequence was repeated several times, resulting in cumulative applications of MTSEA for the times shown under the peaks of the test responses to ACh. There was no decline in current during the 10-s applications of ACh; the return of the current to baseline began with the wash out of ACh. The peak current was normalized and plotted against the cumulative MTSEA exposure time in the absence (B) and presence (D) of ACh. Solid lines indicate least squares single exponential fits to the data, which yield the pseudo first- and second-order rate constants for the reactions (see materials and methods).

by a factor of 0.3 in the presence of ACh, per unit decrease of negative charge. The rate constants for MTSEH increased by a factor of 3.1 in the absence and 5.6 in the presence of ACh, per unit decrease of negative charge.

The increase in the rate constant for MTSEH, as the magnitude of the negative ring charge decreased, was ascribed to an increase in the local pH and a concomitant increase in the probability of the target αT244C sulfhydryl being in the reactive -S^- deprotonated state (see DISCUSSION). The changes in the rate constants of the positively charged MTSEA and AEAETS with decrease in the negative charge of the Glu ring were then a combination of (a) a rate increase due to increased deprotonation of the sulfhydryl, and (b) a rate decrease due to decreased interaction of the charged reagents with the Glu ring charge. The rate increase due to
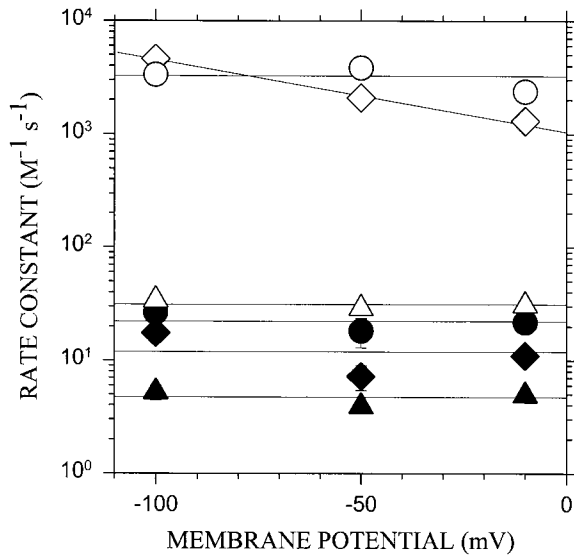
Figure 4. Second-order rate constants for the reactions of thiosulfonate reagents with $\alpha^0{}_2\beta^0\gamma^0\delta^-$ as a function of the transmembrane potential. The rate constants were determined as in Fig. 2 for MTSEH (triangle), MTSEA (circle), and AEAETS (diamond) in the absence (filled symbols) and presence (unfilled symbols) of ACh, at various holding potentials. In each case, the mean ± SEM is plotted for recordings from three to four cells.

deprotonation of the SH should be equal for the charged and uncharged reagents, and this factor should cancel in the ratio of the rate constant of a charged reagent to the rate constant of the uncharged reagent. What remains is due to the interaction of the charged reagent with the intrinsic electrostatic potential.

Intrinsic Electrostatic Potential

As previously noted (Pascual and Karlin, 1998), we calculate the intrinsic electrostatic potential in the vicinity of a target Cys from the ratio of the rate constants for the reactions of two differently charged reagents with the target Cys (at zero transmembrane potential), divided by the ratio of the rate constants for the reactions of the two reagents with 2-mercaptoethanol in solution (Eq. 6). We assume that all channel-specific contributions to the rate constants, other than the electrostatic interactions of the reagent charge with channel charges, both fixed and induced, are factored out in the first ratio and that any difference in the intrinsic reactivity of the two reagents is factored out on division by the second ratio. In this paper, we plot the results as $z\psi_S$ and as the corresponding $\Delta\Delta G^0$ (Eq. 5).

The ratio of ratios, ρ_0, for the pair MTSEA and MTSEH, decreased as the magnitude of the negative charge in the Glu ring decreased, in both the presence and absence of ACh (Fig. 6 A). The corresponding intrinsic electrostatic potential in the vicinity of the site of reaction, $z\psi_s$, and the corresponding $\Delta\Delta G^0$, increased
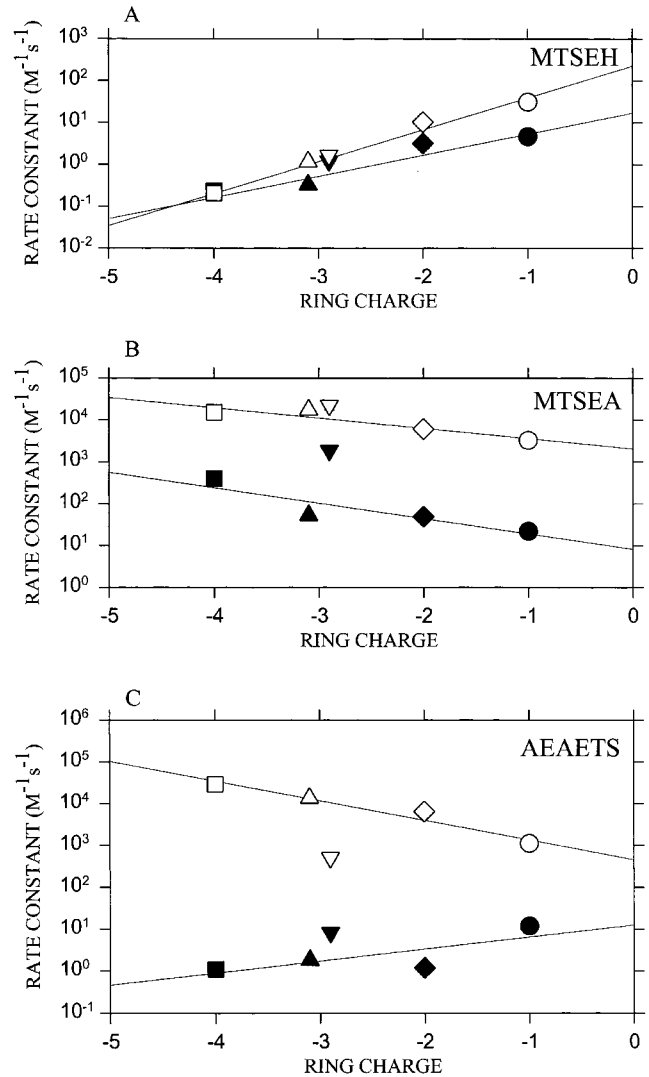

Figure 5. The second-order rate constants for the reaction of thiosulfonate reagents with receptors bearing different ring charges. The rate constants for the reactions at zero transmembrane potential are plotted for MTSEH (A), MTSEA (B), and AEAETS (C) applied both in the absence (filled symbols) and presence (unfilled symbols) of ACh. The correspondence between symbols and subunit combinations is the same as in Fig. 2. The lines are the linear least-squares fits.

linearly (Fig. 6 B). ($z\psi_s$ for $\alpha^-{}_2\beta^-\gamma^0\delta^0$ in the closed state falls off the line, reflecting the deviation of the rate constant for the reaction of MTSEA with this mutant, shown in Fig. 5 B.) The linear least-squares fits yield slopes of 59 mV/ring charge (presence of ACh) and 54 mV/ring charge (absence of ACh). The extrapolated values at zero ring charge are -4 mV (presence of ACh) and 72 mV (absence of ACh). The two lines are nearly parallel, but displaced by 75–100 mV. Remarkably, in the open state of the channel, the intrinsic electrostatic potential in the vicinity of αT244 is almost entirely due to the Glu ring charge.
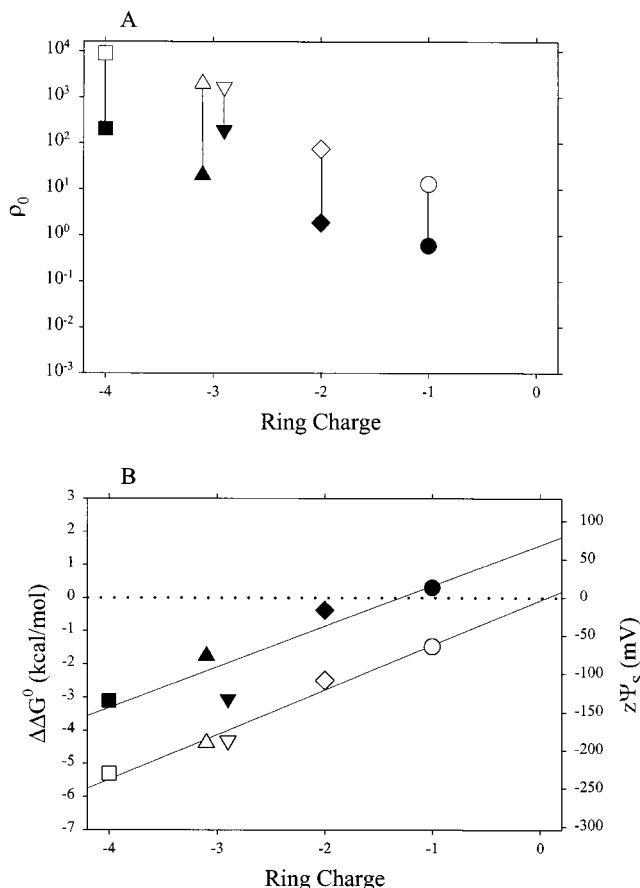
Figure 6. ρ_0 and $\Delta\Delta G^0$ for MTSEA and MTSEH as a function of ring charge. (A) The ratio of the rate constants for the reactions with the receptor was divided by the ratio of the rate constants for the reactions of MTSEA and of MTSEH with 2-mercaptoethanol in solution, thereby normalizing for the difference in the intrinsic reactivities of the two reagents (Pascual and Karlin, 1998). This ratio of ratios, ρ_0, is plotted versus the ring charge. Rate constants for the reactions of the mutant receptors in the presence (unfilled symbols) and absence (filled symbols) of ACh, at zero transmembrane potential, are from the data in Fig. 5. The symbols correspond to the same combinations of subunits as in Fig. 2. (B) $\Delta\Delta G^0$ was calculated as $-RT\ln(\rho_0)$ and $z\psi_s$ was calculated as $\Delta\Delta G^0/F$.

The ratio of ratios, ρ_0, for the pair AEAETS and MTSEH, also decreased as the magnitude of the negative charge in the Glu ring decreased, markedly in the presence but only slightly in the absence of ACh (Fig. 7 A). The corresponding $z\psi_s$, increased linearly (Fig. 7 B). ($z\psi_s$ for $\alpha^-_2\beta^-\gamma^0\delta^0$ is again somewhat anomalous, but in this case in the open state, reflecting the deviation of the rate constant, shown in Fig. 5 C.) The linear least-squares fits yield slopes of 62 mV/charge (presence of ACh) and 14 mV/charge (absence of ACh). The extrapolated values at zero ring charge are 80 mV (presence of ACh) and 92 mV (absence of ACh). In this case, the two lines are not parallel, but rather nearly converge at zero ring charge.
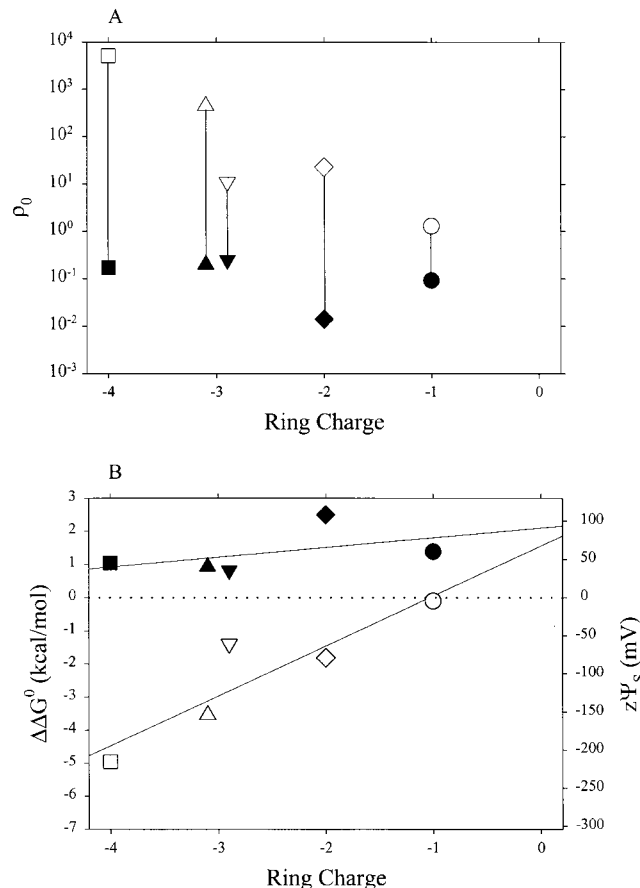
Figure 7. ρ_0 (A) and $\Delta\Delta G^0$ and $z\psi_s$ (B) for AEAETS and MTSEH. The details are as in Fig. 6.

For the pseudo wild-type receptor ($\alpha^-_2\beta^-\gamma^0\delta^-$, ring charge -4), the values of $z\psi_s$ and $\Delta\Delta G^0$ determined with AEAETS and MTSEH (-215 and -5.0 kcal/mol) and those determined with MTSEA and MTSEH (-230 and -5.3 kcal/mol) are nearly the same. At first glance, this is surprising given that the charge of AEAETS is $+2$ and the charge of MSTEA is $+1$. A theoretical calculation discussed below indicates that the second positively charged ammonium of AEAETS, located ~10 Å away from the first positively charged ammonium and from the ring of charged glutamates, may have little net effect on ΔG^0 for the association of AEAETS with the site of reaction in the channel and hence little effect on $\Delta\Delta G^0$ and $z\psi_s$.

Lysine Ring Charge

Adjacent to the ring of four Glu and a Gln is a ring of five Lys (Fig. 1 C). Mutations in these Lys have been made previously, and the mutants that were functional did not show marked changes in conductance or other properties (Imoto et al., 1988; Wilson and Karlin, 1998; Corringer et al., 1999). We tested whether changing the total charge in the lysine ring affected the intrinsic

electrostatic potential. We mutated βK253 to Glu and expressed this mutant together with αT244C, wild-type γ, and wild-type δ. The total charge in the lysine ring was thereby changed from +5 to +3. The charge in the Glu ring remained −4. ψ_S was estimated with the pair MTSEA and MTSEH in the presence and absence of ACh. $z\psi_S$ for βK253E in the presence of ACh was 31 mV less negative, and in the absence of ACh, 15 mV less negative than ψ_S for the pseudo wild type, $\alpha^-{}_2\beta^-\gamma^0\delta^-$. $z\psi_S$ was also estimated with the pair AEAETS and MT-SEH. $z\psi_S$ for βK253E was 56 mV less negative in the presence of ACh, and 16 mV more positive in the absence of ACh, than ψ_S for $\alpha^-{}_2\beta^-\gamma^0\delta^-$. Thus, in all cases, making the charge in the ring of Lys less positive changed $z\psi_S$ modestly in the positive direction. This direction is the opposite of what we would expect if the charges in the ring of Lys interacted directly with cations in the channel.

DISCUSSION

Using an approach (Stauffer and Karlin, 1994; Pascual and Karlin, 1998) that is an elaboration of the substituted-cysteine-accessibility method (Akabas et al., 1992, 1994), we have estimated the intrinsic electrostatic potential in the narrowest part of the ACh receptor channel. In both the open and closed states of the channel, this potential is linearly dependent on the number of Glu in the intermediate ring of charge. We discuss below the relationship of our estimation of the intrinsic electrostatic potential to the free energy of association of reagents in bulk solution with the site of reaction in the channel, the validation by the current results of the assumptions of our approach, the effect of the intrinsic electrostatic potential on the acid dissociation and, thereby, the reactivity of the target Cys, and the implications for cation conductance of the large negative electrostatic potential in the region of the selectivity filter.

Estimating the Intrinsic Electrostatic Potential

We estimate ψ_S using Eq. 6, which we derived initially from the simple two-barrier–one-well kinetic model of Woodhull (1973) applied to a reagent species, with the additional condition that the reagent can react covalently with a Cys within the well (or site) (Pascual and Karlin, 1998). The reagent is added to one side of the membrane, and we assume that its concentration on the other side of the membrane during short applications is negligible. The observed rate constant, κ, for the reaction of reagent added, say, to the extracellular side of the membrane depends on four reaction rate constants; these characterize the transfer from the extracellular side to the site (i.e., association with the site), the transfer from the site back to the extracellular side, the transfer from the site to the intracellular side,

and the covalent reaction between reagents associated with the site and the Cys in the site. The rate constant for the transfer from the intracellular side to the site is eliminated because the reagent concentration on the intracellular side is close to zero.

When the rate constant for transfer of reagent from the site back to the extracellular side is much greater than both the rate constant for transfer from the site to the intracellular side and the rate constant for reaction at the site, the reagent at the site is close to equilibrium with reagent in the extracellular solution. Also, as we know from the absence of reversible channel-blocking by the reagents at the concentrations used here, the degree of occupation of the reaction site is low; i.e., the rate constant for transfer of reagent from the site back to the extracellular side is much greater than the rate constant for transfer of reagent from the extracellular side to the site times the extracellular concentration. Under these conditions, the concentration of sites occupied by reagent is approximately equal to the total concentration of not-yet-reacted sites times the equilibrium affinity constant times the extracellular reagent concentration, and the second-order rate constant for the reaction of the site, κ, is the intrinsic rate constant for the reaction of the occupied site times the equilibrium affinity constant (see Pascual and Karlin, 1998). The equilibrium affinity constant equals $\exp(-\Delta G^0/RT)$, where ΔG^0, the standard free energy of association (or transfer) was defined in MATERIALS AND METHODS; i.e., $\kappa \cong k_S \exp(-\Delta G^0/RT)$.

For two reagents, 1 and 2, that are similar except for their charges, we form the ratio, $^1\kappa/^2\kappa \cong (^1k_S/^2k_S) \exp(-\Delta\Delta G^0/RT)$. We assume that the ratio of the rate constants for the reactions of the reagents with the Cys in the site, $^1k_S/^2k_S$, is the same as the ratio of the rate constants for their reactions with a simple thiol, 2-mercaptoethanol, in bulk solution; i.e., $^1k_S/^2k_S = ^1k_{ME}/^2k_{ME}$. With ρ_0 defined by Eq. 4, Eq. 5 follows. We also assume that the only contributions to $\Delta\Delta G^0$ that do not cancel are those due to the difference in the charges of the two reagents; i.e., $\Delta\Delta G^0$ is just the difference in the electrostatic free energies of association of the two reagents with the site of reaction. The more similar the two reagents, the smaller the errors in these two assumptions. The reaction mechanisms of the three reagents used here, MTSEA, AEAETS, and MTSEH, are the same. MTSEA is also very similar in size and shape to MTSEH; however, the doubly charged AEAETS is significantly longer than MTSEH (13 compared with 10 Å). For the more reliable pair, MTSEA and MTSEH, $\Delta\Delta G^0$ is the difference in the free energies of association with the site of the positively charged ammonium head group of MTSEA and of the neutral hydroxyl head group of MTSEH.

Neglecting any differences in the nonelectrostatic

contributions to the binding of an ammonium group and a hydroxyl group, we equate $\Delta\Delta G^0$ to $(z_1 - z_2) F\psi_S$; i.e., to $F\psi_S$ for $z_1 = 1$ and $z_2 = 0$. The electrostatic free energy of transfer of a charged reagent from bulk solution to a site in the channel would have the form $zF\psi_S$, however, if ψ_S were due to fixed charges only and independent of the reagent charge z. Because there are dielectric boundaries in the system, the free energy of transfer also contains a term equal to $0.5\ zF\psi_{\text{Dielectric}}$, where $\psi_{\text{Dielectric}}$ is the potential due to the reaction field generated by the reagent charge.[3] The electrostatic potential at the position of the reagent charge due to all other fixed charges and to dielectric boundaries is $\psi_S' = \psi_{\text{Fixed}} + \psi_{\text{Dielectric}}$; however, $\Delta\Delta G^0 = (z_1 - z_2)F(\psi_{\text{Fixed}} + 0.5\ \psi_{\text{Dielectric}})$, and we do not have separate measurements of ψ_{Fixed} and $\psi_{\text{Dielectric}}$. Thus, ψ_S, calculated as $\Delta\Delta G^0/[(z_1 - z_2)F]$, equals $\psi_{\text{Fixed}} + 0.5\ \psi_{\text{Dielectric}}$ and differs from ψ_S' by $0.5\ \psi_{\text{Dielectric}}$. In the theoretical calculations discussed below, $\psi_{\text{Dielectric}}$ is much smaller than ψ_{Fixed}, so that $\psi_S \approx \psi_S'$.

In equating the electrostatic free energy of transfer to $zF\psi_S$, we assume that the charge of the reagent is at a unique location and electrostatic potential. This is valid for MTSEA ($z_1 = +1$), but not for AEAETS, which has two ammonium groups separated by as much as 10 Å. When the ether sulfur of AEAETS is in position to react with the Cys of αT244C, one positively charged ammonium group is close to αE241 and the other glutamates in the intermediate ring while the other positively charged ammonium is at the level of αS248. From previous measurements of ψ_S at different positions in the channel (Pascual and Karlin, 1998), the magnitude of the negative potential at the second ammonium group would be considerably less than at the first.

Because the two charges on AEAETS are separated, $\Delta\Delta G^0$ for the pair AEAETS and MTSEH, with a charge difference of $+2$, is not twice the magnitude of $\Delta\Delta G^0$ for the pair MTSEA and MTSEH, with a charge difference of $+1$. The experimentally derived values of $\Delta\Delta G^0$ for the two pairs of reagents in the open channel were almost identical (Figs. 6 B and 7 B).

The unequal contributions of the two charges of AEAETS are rationalized by a theoretical analysis of a simplified model of the channel (Fig. 8). In the open channel with a ring charge of -4, we calculate that $\Delta\Delta G^0$ for the pair AEAETS and MTSEH is $1.4\times$ $\Delta\Delta G^0$ for the pair MTSEA and MTSEH (Fig. 9 A), not $2\times$. This result can be explained as follows: the ammonium group of MTSEA and one of the ammonium groups of AEAETS sit in the plane of the negative charges (representing the ring of Glu) when the ether sulfur is in position to react

with the Cys. The electrostatic free energies for the transfer of these ammonium groups from bulk solution to their position in the channel are the same for the two reagents. The electrostatic free energy for the transfer of the second ammonium of AEAETS, however, is less favorable than the first because the second ammonium is farther from the ring of negative charges and is further from bulk water at the end of the channel. In general, the electrostatic free energies of transfer of spatially separated charges are unlikely to be equal. To avoid the uncertainty in the appropriate value of z to use for AEAETS in Eq. 6, we calculate instead $z\psi_S$ ($= \Delta\Delta G^0/F$) for both pairs of reagents (Figs. 6 B and 7 B).

$z\psi_S$ and the Glutamate Ring Charge

Receptor complexes with Glu ring charges of -4, -3, -2, and -1 were probed with MTSEA, MTSEH, and AEAETS. Based on the rate constants for the reactions of MTSEA and MTSEH with αT244C in the presence of a near-saturating concentration of ACh (the open state[4]), $z\psi_S$ increased linearly in a positive direction from -230 mV at a ring charge of -4 to the extrapolated value of -4 mV at a ring charge of 0 (Fig. 6 B). The linear increase with ring charge indicates that $z\psi_S$ and $\Delta\Delta G^0$ are electrostatic in origin and that the conditions on Eqs. 5 and 6 are not seriously violated. The extrapolation of $z\psi_S$ at 0 ring charge to close to 0 mV indicates that in the open state, at least, the Glu ring is the only net source of $z\psi_S$. The contributions of all other charges, fixed or induced, balance.

Theoretical calculation of $z\psi_S$ based on MTSEA and MTSEH in the open state gave values that corresponded closely to the experimental values (Fig. 9 A). In the model, there are no fixed charges other than the ring of charges representing the Glu. When these charges, and thereby ψ_{Fixed}, are eliminated, the only component of the electrostatic potential is $\psi_{\text{Dielectric}}$. With the charge of MTSEA close to the end of the channel, as in the model, $\psi_{\text{Dielectric}}$ (calculated with the ring

---

[3]Because $\psi_{\text{Dielectric}}$ depends on z, $0.5\ zF\psi_{\text{Dielectric}}$ is proportional to 0.5 z^2, and only if $\psi_{\text{Fixed}} >> \psi_{\text{Dielectric}}$ is $\Delta\Delta G^0$ proportional to the first power of the reagent charge, z.

[4]The receptor exists in at least four different functional states, closed, open, and fast- and slow-desensitized. Only in the open state is the channel conducting. As discussed previously (Pascual and Karlin, 1998), reagents added in the absence of ACh react predominantly with the closed state, and during brief ($\leq$20 s) application of reagent together with ACh the reaction is with a mixture of receptors in the open state and with receptors in the fast-desensitized state. In the case of reactions with αT244C, the rate constant for the reaction of MTSEA with receptor that has been driven into the slow-desensitized state is two to three orders of magnitude smaller than with receptor in the mixed open and fast-desensitized states (our unpublished results). Furthermore, the dependence on transmembrane potential of the rate of reaction of αT244C with AEAETS in the presence of ACh suggests that the reaction is predominantly with receptor in the conducting open state, and not with receptor in the closed state or in either of the nonconducting desensitized states. For convenience, we call the mixed state within the first 20 s of ACh application the open state.
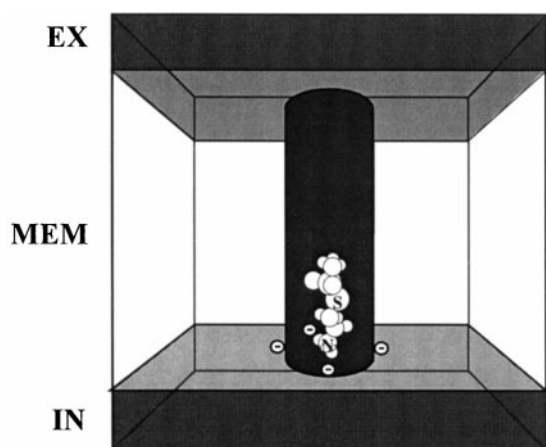
Figure 8. A simple model of the open channel. A cylindrical pore of 8-Å diameter and 30-Å length crosses a slab representing the bilayer and the bilayer-embedded receptor. Water is on either side of the slab and within the channel (dark fill). The water has a dielectric constant of 80, and the slab (no fill) has a dielectric constant of 2. Measuring along the long axis (x axis) of the channel from its midpoint, the intracellular end is at x = −15 Å and the extracellular end is at x = 15 Å. Point charges are placed at the vertices of a pentagon at x = −14 Å and at a distance from the x axis (r coordinate) of 5 Å. A model of MTSEA is shown in the channel with the positively charged ammonium centered at r = 0 Å, x = −14 Å. The point charges were given values of −1 or 0. The closed channel includes as a gate, a disc of dielectric constant 2, 8-Å diameter and 2-Å thick, from x = −12 to −14 Å. EX, extracellular; IN, intracellular; MEM, membrane.

Figure 9. Electrostatic free energies of transfer into the model channel. (A). The differences ($\Delta\Delta G^0$) in the ΔG^0 of MTSEA and MTSEH (circles) and of AEAETS and MTSEH (diamonds) are shown for both the open (unfilled symbols) and closed (filled symbols) states. In the open state, MTSEA was oriented as in Fig. 8, with the ammonium N at x = −14 Å, r = 0 Å. The ammonium of AEAETS closest to the -S⁻ was placed at r = 0 Å and x = −14 Å, and the second ammonium closest to the -SO₂⁻ was at r = 0 Å and x = −4.4 Å. The hydroxyl hydrogen of MTSEH was placed in the same location as the ammonium of MTSEA, and the orientation of the molecule was similar. In the closed state, the head groups of the reagents were moved to x = −10 Å, while the orientations were unchanged. (B). ΔG^0 for the transfer of a Na^+ from the extracellular solution to the channel was calculated at 1-Å intervals, from x = −18 to 18 Å. (The channel extends from −15 to 15 Å.) In the closed state, the Na^+ was excluded from the gate, which extends from x = −14 to −12 Å (double-headed arrow).

charge equal to zero) is close to zero. We do not know the actual magnitude of $\psi_{Dielectric}$ when MTSEA is in the lumen of the receptor. If $\psi_{Dielectric}$ is not close to 0, then ψ_{Fixed} due to fixed charges other than the intermediate ring Glu must be half the magnitude of $\psi_{Dielectric}$ and opposite in sign to yield the overall ψ_S close to zero.

In the closed state[4] of the receptor, $z\psi_S$ determined with MTSEA and MTSEH also increased linearly as the negative ring charge was decreased, and the fitted line was parallel to the line fitted to the open state data, displaced by 74 mV in the positive direction at a ring charge of 0 (Fig. 6 B). This difference between the closed and open states is consistent with a gate closing between the Glu ring and the target Cys substituted for αT244 (Wilson and Karlin, 1998), thereby keeping the ammonium group farther from the Glu ring and decreasing the effective dielectric constant in the lumen. In the theoretical model (Fig. 8), the gate was represented by a 2-Å-thick disk with dielectric constant 2. The calculated $z\psi_S$ and $\Delta\Delta G^0$ for the pair MTSEA and MTSEH were similar to the experimental values at ring charge −4; however, the theoretical values rose more quickly than the experimental values as the magnitude of the ring charge approached zero (Fig. 9 A). This discrepancy is likely a consequence of the over-simplified gate in the model, which, although appropriately located between the ring of charge and αT244, occludes
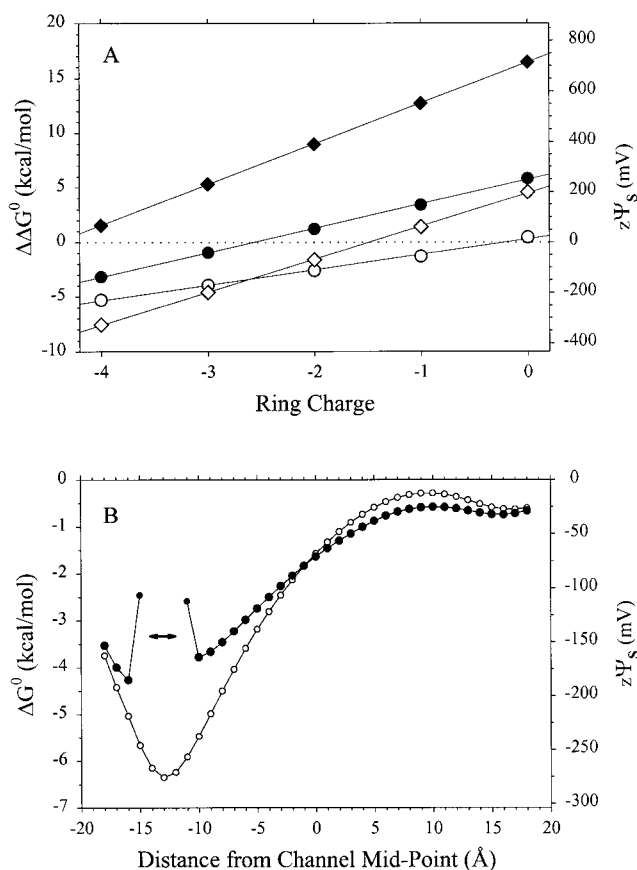
the channel more than would be necessary to block the passage of alkali metal ions.[5]

Determined with the pair AEAETS and MTSEH, $z\psi_S$ in the open state once again increased linearly with the decrease in the magnitude of the ring charge (Fig. 7 B), generally supporting the electrostatic basis of $z\psi_S$. In this

---

[5]In the future, we will explore the theoretical implications of more subtle gate structures, of a more realistic lumen geometry, of moving the intermediate ring, of including the inner and outer rings of charges and the ring of lysines, and of varying the orientation of the reagents in the channel.

case, $z\psi_S$ did not extrapolate to $\sim$0 mV at 0 ring charge. Also, in the closed state, $z\psi_S$ was positive at all values of the ring charge. Both phenomena are seen in the theoretical model (Fig. 9 A). In the closed state, however, the slope of the line fitted to the experimental $z\psi_S$ was not significantly different from 0. AEAETS is larger than MTSEH and, because of its greater size, the narrow channel could retard its reaction much more than that of MTSEH. If channel closing involves a narrowing of the lumen from αG240 to αT244 (Wilson and Karlin, 1998), the reaction of AEAETS with αT244C in the closed state could be severely hindered. In this case, nonelectrostatic contributions might not be eliminated in ρ_0 and might indeed dominate over the electrostatic contributions.

One question is whether the changes in ρ_0 with changes in ring charge could have been due to changes in gating kinetics. The mutations resulted in as much as a fourfold increase in the EC$_{50}$ for ACh (Fig. 2 B). The changes were likely the results of changes in gating kinetics, which might have affected the rates of reaction of the reagents in the presence of ACh. There was no correlation, however, between the EC$_{50}$ of the different mutants and the rate constants for the reactions of MTSEA or of AEAETS (plot not shown). The rate constants for MTSEH increased, albeit nonlinearly, as the EC$_{50}$ increased; however, this could not be due to changes in gating because in most mutants the rate constants for MTSEH were nearly the same in the open and closed states (Fig. 5 A). Thus, the changes in ρ_0 and $z\psi_S$ with changes in the Glu ring charge were not due to changes in gating kinetics.

We conclude that in the open state of the channel the intrinsic electrostatic potential in the vicinity of αT244 is largely due to the negatively charged Glu in the intermediate ring of charge. All other electrostatic interactions with the reagents and, presumably, with permeant inorganic cations must more or less balance.

Reaction Rate Constants of MTSEH and the Glu Ring Charge

Methanethiosulfonates react at least 5×10^9 faster with dissociated thiolates (RS$^-$) than with undissociated thiols (RSH) (Roberts et al., 1986). Essentially all reaction is with the thiolate. Thus, the rate constant for the reaction of the target Cys in αT244C depends on, among other factors, the ionization of the thiol. The increase in the rate constant for neutral MTSEH as the magnitude of the negative ring charge decreased (Fig. 5A), we ascribe to an increase in the local pH and a concomitant increase in the probability of the target αT244C sulfhydryl being in the reactive -S$^-$ deprotonated state. This can be modeled by assuming that the proton concentration, h_S, in the vicinity of the Cys is at equilibrium with the extramembranous proton concentration, h_E, according to a Boltzmann distribution, $h_S/h_E = \exp(-\Delta G^0_{S*H}/$

$RT)$, ΔG^0_{S*H} is the standard free energy of transfer of a proton from the extramembranous solution to the vicinity of the target Cys when the reagent is also in the channel in position to react; i.e., $\Delta G^0_{S*H} = G^0_{S*H} - G^0_{S*} - G^0_H$, where G^0_{S*H} is the standard free energy of the proton in the site also occupied by reagent, G^0_{S*} is the standard free energy of the site occupied by reagent, but not a proton, and G^0_H is the standard free energy of the proton in bulk solution. We can define an electrostatic potential, $\psi_{S*} = \Delta G^0_{S*H}/F$. Note that ΔG^0_{S*H} is different than $\Delta\Delta G^0$ in Eq. 6, and ψ_{S*} is different than ψ_S.

For MTSEH, for which $z = 0$, the observed rate constant for the modification of the Cys, κ, is given by Eq. 7 in Pascual and Karlin (1998), which we write as $\kappa = k_S k'$, where k_S is the rate constant for the reaction of MTSEH at the site with the Cys, and k' is an expression containing the transfer rate constants, which do not vary with electrostatic potential because MTSEH is neutral. The rate constant k_S applies to the rate of reaction of the target Cys in terms of the total concentration of the Cys. Only a small fraction of the Cys is in the reactive thiolate form. If k^- is the rate constant for the reaction of the thiolate form with MTSEH at the site, then $k_S = (k^- K_A/h_E)\exp(F\psi_{S*}/RT)$, where K_A is the acid dissociation constant of the Cys sulfhydryl. The observed overall rate constant, κ, is then given by $\kappa = (k'k^- K_A/h_E)\exp(F\psi_{S*}/RT)$ and $\ln(\kappa) = \ln(k'k^- K_A/h_E) + F\psi_{S*}/RT$.

For uncharged MTSEH, only ψ_{S*} is a function of q, the ring charge. Furthermore, the experimental $\ln(\kappa)$ versus ring charge is well fit by a straight line (Fig. 5 A). Thus, ψ_{S*} is a linear function of q, i.e., $\psi_{S*} = mq + b$. The slopes of the least-squares lines in Fig. 5 A imply that m is 43 mV/ring charge in the open state and 27 mV/ring charge in the closed state. The comparable slopes of ψ_S, determined with the pair MTSEA and MTSEH, as a function of q, were 59 mV/ring charge in the open state and 54 mV/ring charge in the closed state (Fig. 6 B). The linear relationships between $\ln(\kappa)$ and q for the reaction of MTSEH are comparable to the linear relationships between ψ_S and q, determined with MTSEA and MTSEH. This correspondence supports the notion that the ring of Glu exerts an electrostatic effect in the channel lumen at the level of αT244.

The actual pH in the channel lumen is not known. If it were low enough around the Glu, then it would seem unlikely that all four Glu carboxyls would be deprotonated simultaneously. Nevertheless, each step of Glu mutation to Gln has an equivalent effect on ψ_S (Fig. 6 B), consistent with all four Glu being ionized, at least while reagent is in the site.

Lysines

Adjacent to the ring of Glu is a ring of five Lys, one residue closer in the sequence to the target Cys in αT244C. Mutation of one of these Lys to Glu, in βK252E, had a

paradoxical effect on ψ_S. Even though the charge in this ring was made less positive by 2 charges, ψ_S in the open state in this mutant was more positive by ~ 30 mV than in the pseudo wild type. The direction of change is opposite to that which would result from a direct interaction of the Lys residues with the charge of the reagents. The magnitude of this change is also small compared with the change in ψ_S caused by a change of 2 charges in the Glu ring (Fig. 6 B).

Despite this indication that the Lys do not interact directly with the reagents, when αK242 was mutated to a Cys and expressed with wild-type β, γ, and δ subunits in HEK 293 cells, the Cys reacted in the open state (but not in the closed state) of the channel with MTSEA added either extra- or intracellularly (Wilson and Karlin, 1998). Thus, the Cys was accessible in the open channel. It is possible that the αK242 and the aligned Lys in the other subunits do not ordinarily face the channel in wild-type receptor and play primarily a structural role. It is possible that the side chains are so oriented that even though the lysines are one residue closer in the sequence than the glutamates to the target Cys in αT244C, the ϵ-NH$_3^+$ of the Lys side chains are considerably farther from the target Cys than the γ-COO$^-$ of the glutamates.

Supporting this interpretation is the previous finding that the mutation of the homologous Lys to Glu in Torpedo ACh receptor β, γ, or δ subunits had no effect on the conductance of this receptor (Imoto et al., 1988). Also, in a neuronal ACh receptor, the homomeric $(\alpha 7)_5$, the combination of neutralization of the Glu ring and two additional mutations was sufficient to change the charge selectivity of the channel from cationic to anionic, albeit severely reducing the ACh-induced current. Further mutation to neutralize the Lys ring, however, did not alter the anionic selectivity or the current (Corringer et al., 1999), again indicating that the Lys do not interact significantly with ions in the channel.

Two other channel-flanking rings of net negative charge, the outer ring of residues aligned with αE262 and the inner ring aligned with αD238, contribute to the conductance of the muscle-type ACh receptor channel, but considerably less than does the intermediate ring of charge (Imoto et al., 1988). Also, in the neuronal $(\alpha 7)_5$ channel, neutralization of the inner ring of charge had no detectable effects on ACh-evoked currents (Corringer et al., 1999). The Glu in the intermediate ring of charge are the major charged contributors to cation conductance (Imoto et al., 1988) and to the intrinsic electrostatic potential.

Implications for Conductance of Alkali Metal Ions

Cation conductance through the ACh receptor is linearly dependent on the number of charged residues in the intermediate ring of charge (Imoto et al., 1988). The Glu in the intermediate ring are likely to be in the narrowest part of the channel, which extends from αG240 to αT244 (Wilson and Karlin, 1998). This region includes the selectivity filter (Imoto et al., 1991; Konno et al., 1991; Villarroel et al., 1991, 1992; Cohen et al., 1992) and the activation gate (Wilson and Karlin, 1998; but see Miyazawa et al., 1999). This is presumably the region of the channel previously inferred to be short and narrow (Dani, 1989) and to contain the singly occupied, principal cation-binding site (Dani and Eisenman, 1987). Cations moving through this region are partially dehydrated. In this region of the open channel, the electrostatic contribution to $\Delta\Delta G^0$ and the equivalent $z\psi_S$, measured with the pair MTSEA and MTSEH, are -5.3 kcal/mol and -230 mV.

We also calculated $\Delta\Delta G^0$ and the equivalent $z\psi_S$ in a cylindrical model of the channel (Fig. 8), which is highly simplified compared with a moderate-resolution structure of the open ACh receptor channel (Unwin, 1995; Adcock et al., 1998). The simple cylindrical model with a ring charge of -4 gave values for $\Delta\Delta G^0$ and $z\psi_S$ very close to the experimental ones (Fig. 9 A).

In addition, we calculated the electrostatic contribution to ΔG^0, and $z\psi_S$ for the transfer of a Na$^+$ from the extracellular solution to various positions along the axis of the model channel (Fig. 9 B). The electrostatic contribution to ΔG^0 and $z\psi_S$ reach minima of -6.3 kcal/mol and -273 mV at a distance from the channel midpoint of -13 Å (i.e., 2 Å from the intracellular end of the model channel). By comparison, the electrostatic contribution to the free energy of transfer of a K$^+$ from bulk water to the central cavity of the KcsA potassium channel was calculated to be -8.5 kcal/mol (Roux and MacKinnon, 1999).

In the ACh receptor channel, the large negative electrostatic potential could be the basis for a high affinity cation-binding site in the vicinity of the intermediate ring. We cannot calculate an equilibrium binding constant, however, because neither the experimentally derived $\Delta\Delta G^0$ for the pair MTSEA and MTSEH nor the theoretically calculated electrostatic contribution to ΔG^0 for the transfer of a Na$^+$ is equivalent to the total free energy of transfer of a cation from bulk solution to the channel site.[6] If, however, the free energy of cation

---

[6]Even if the ammonium group of MTSEA were representative of a permeant cation and the hydroxyl group of MTSEH were representative of a water molecule displaced by the cation, $\Delta\Delta G^0$ does not include the entropy of transfer of the cation from bulk solution to the site, the value of which is unknown. The calculated electrostatic contribution to ΔG^0 for the transfer of Na$^+$ from bulk solution to the site is the electrostatic contribution to the enthalpy of transfer. It does not include van der Waals contributions to the enthalpy of transfer and does not include the entropy of transfer.

transfer were in the range of −5 to −6 kcal/mol, the equivalent equilibrium dissociation constant would be in the range of 40–200 μM, far lower than the half-saturation concentration for Na$^+$ conductance of ∼100 mM (Dani and Eisenman, 1987). Although the detailed physical mechanisms of cation selectivity and transport through the ACh receptor channel are not known (Dani and Levitt, 1990), the large, negative electrostatic potential, arising from the intermediate ring of charge, likely plays a central role in both selectivity and transport.

REFERENCES

Adcock, C., G. Smith, and M. Sansom. 1998. Electrostatics and the ion selectivity of ligand-gated channels. *Biophys. J.* 75:1211–1222.

Akabas, M.H., C. Kaufmann, P. Archdeacon, and A. Karlin. 1994. Identification of acetylcholine receptor channel-lining residues in the entire M2 segment of the alpha subunit. *Neuron.* 13:919–927.

Akabas, M.H., D.A. Stauffer, M. Xu, and A. Karlin. 1992. Acetylcholine receptor channel structure probed in cysteine-substitution mutants. *Science.* 258:307–310.

Andersen, O.S., and R.E.D. Koeppe. 1992. Molecular determinants of channel function. *Physiol. Rev.* 72:S89–158.

Brooks, B.R., R.E. Bruccoleri, B.D. Olafson, D.J. States, S. Swaminathan, and M. Karplus. 1983. CHARMM: a program for macromolecular energy minimization and dynamics calculation. *J. Comput. Chem.* 4:187–217.

Cohen, B.N., C. Labarca, N. Davidson, and H.A. Lester. 1992. Mutations in M2 alter the selectivity of the mouse nicotinic acetylcholine receptor for organic and alkali metal cations. *J. Gen. Physiol.* 100:373–400.

Corringer, P.J., S. Bertrand, J.L. Galzi, A. Devillers-Thiery, J.P. Changeux, and D. Bertrand. 1999. Mutational analysis of the charge selectivity filter of the alpha7 nicotinic acetylcholine receptor. *Neuron.* 22:831–843.

Corringer, P.-J., N. Le Novere, and J.-P. Changeux. 2000. Nicotinic receptors at the amino acid level. *Ann. Rev. Pharmacol. Toxicol.* In press.

Dani, J.A. 1989. Open channel structure and ion binding sites of the nicotinic acetylcholine receptor channel. *J. Neurosci.* 9:884–892.

Dani, J.A., and G. Eisenman. 1987. Monovalent and divalent cation permeation in acetylcholine receptor channels. Ion transport related to structure. *J. Gen. Physiol.* 89:959–983.

Dani, J.A., and D.G. Levitt. 1990. Diffusion and kinetic approaches to describe permeation in ionic channels. *J. Theor. Biol.* 146:289–301.

Doyle, D.A., J. Morais Cabral, R.A. Pfuetzner, A. Kuo, J.M. Gulbis, S.L. Cohen, B.T. Chait, and R. MacKinnon. 1998. The structure of the potassium channel: molecular basis of K+ conduction and selectivity. *Science.* 280:69–77.

Eisenberg, R. 1996. Computing the field in proteins and channels. *J. Membr. Biol.* 150:1–25.

Gilson, M.K., K.A. Sharp, and B.H. Honig. 1987. Calculating the electrostatic potential of molecules in solution: method and error assessment. *J. Comp. Chem.* 9:327–335.

Green, M.E., and J. Lu. 1995. Monte-Carlo simulation of the effects of charges on water and ions in a tapered pore. *J. Colloid Interface Sci.* 171:117–126.

Green, W.N., and O.S. Andersen. 1991. Surface charges and ion channel function. *Annu. Rev. Physiol.* 53:341–359.

Guinamard, R., and M.H. Akabas. 1999. Arg352 is a major determinant of charge selectivity in the cystic fibrosis transmembrane conductance regulator chloride channel. *Biochemistry.* 38:5528–5537.

Hille, B. 1992. Ionic channels of excitable membranes. Sinauer Associates Inc., Sunderland, MA. 607 pp.

Hucho, F., V.I. Tsetlin, and J. Machold. 1996. The emerging three-dimensional structure of a receptor. The nicotinic acetylcholine receptor. *Eur. J. Biochem.* 239:539–557.

Imoto, K., C. Busch, B. Sakmann, M. Mishina, T. Konno, J. Nakai, H. Bujo, Y. Mori, K. Fukuda, and S. Numa. 1988. Rings of negatively charged amino acids determine the acetylcholine receptor channel conductance. *Nature.* 335:645–648.

Imoto, K., T. Konno, J. Nakai, F. Wang, M. Mishina, and S. Numa. 1991. A ring of uncharged polar amino acids as a component of channel constriction in the nicotinic acetylcholine receptor. *FEBS Lett.* 289:193–200.

Karlin, A., and M.H. Akabas. 1995. Toward a structural basis for the function of nicotinic acetylcholine receptors and their cousins. *Neuron.* 15:1231–1244.

Karlin, A., and M.H. Akabas. 1998. Substituted-cysteine-accessibility method. *In* Methods in Enzymology. Vol. 293. P.M. Conn, editor. Academic Press, Inc., San Diego, CA. 123–145.

Konno, T., C. Busch, E. Von Kitzing, K. Imoto, F. Wang, J. Nakai, M. Mishina, S. Numa, and B. Sakmann. 1991. Rings of anionic amino acids as structural determinants of ion selectivity in the acetylcholine receptor channel. *Proc. R. Soc. Lond. B Biol. Sci.* 244:69–79.

Leonard, R.J., C.G. Labarca, P. Charnet, N. Davidson, and H.A. Lester. 1988. Evidence that the M2 membrane-spanning region lines the ion channel pore of the nicotinic receptor. *Science.* 242:1578–1581.

Mackerell, A.D., D. Bashford, M. Bellot, R.L.J. Bunbrack, M.J. Field, S. Fisher, J. Gao, H. Guo, S. Ha, D. Joseph, et al. 1992. Self-consistent parameterization of biomolecules for molecular modeling and condensed phase simulation. *Biophys. J.* 61:A143.

Miyazawa, A., Y. Fujiyoshi, M. Stowell, and N. Unwin. 1999. Nicotinic acetylcholine receptor at 4.6 A resolution: transverse tunnels in the channel wall. *J. Mol. Biol.* 288:765–786.

Parsegian, A. 1969. Energy of an ion crossing a low dielectric membrane: solutions to four relevant electrostatic problems. *Nature.* 221:844–846.

Pascual, J.M., and A. Karlin. 1998. State-dependent accessibility and electrostatic potential in the channel of the acetylcholine receptor: inferences from rates of reaction of thiosulfonates with substituted cysteines in the M2 segment of the alpha subunit. *J. Gen. Physiol.* 111:717–739.

Rashin, A.A., and B. Honig. 1985. Reevaluation of the Born model of ion hydration. *J. Phys. Chem.* 89:5588–5593.

Roberts, D.D., S.D. Lewis, D.P. Ballou, S.T. Olson, and J.A. Shafer. 1986. Reactivity of small thiolate anions and cysteine-25 in papain toward methyl methanethiosulfonate. *Biochemistry.* 25:5595–5601.

Roux, B., and M. Karplus. 1994. Molecular dynamics simulations of

the gramicidin channel. *Annu. Rev. Biophys. Biomol. Struct.* 23: 731–761.

Roux, B., and R. MacKinnon. 1999. The cavity and pore helices in the KcsA K$^+$ channel: electrostatic stabilization of monovalent cations. *Science.* 285:100–102.

Sharp, K.A., and B.H. Honig. 1990. Calculating total electrostatic energies with the nonlinear Poisson-Boltzmann equation. *J. Phys. Chem.* 94:7684–7692.

Sitkoff, D., K.A. Sharp, and B. Honig. 1994. Accurate calculation of hydration free energies using macroscopic solvent models. *J. Phys. Chem.* 98:1978–1988.

Stauffer, D.A., and A. Karlin. 1994. Electrostatic potential of the acetylcholine binding sites in the nicotinic receptor probed by reactions of binding-site cysteines with charged methanethiosulfonates. *Biochemistry.* 33:6840–6849.

Syganow, A., and E. von Kitzing. 1995. Integral weak diffusion and diffusion approximations applied to ion transport through biological ion channels. *J. Phys. Chem.* 99:12030–12040.

Unwin, N. 1995. Acetylcholine receptor channel imaged in the open state. *Nature.* 373:37–43.

Villarroel, A., S. Herlitze, M. Koenen, and B. Sakmann. 1991. Location of a threonine residue in the alpha-subunit M2 transmembrane segment that determines the ion flow through the acetylcholine receptor channel. *Proc. R. Soc. Lond. B Biol. Sci.* 243:69–74.

Villarroel, A., S. Herlitze, V. Witzemann, M. Koenen, and B. Sakmann. 1992. Asymmetry of the rat acetylcholine receptor subunits in the narrow region of the pore. *Proc. R. Soc. Lond. B Biol. Sci.* 249:317–324.

Wilson, G.G., and A. Karlin. 1998. The location of the gate in the acetylcholine receptor channel. *Neuron.* 20:1269–1281.

Woodhull, A.M. 1973. Ionic blockage of sodium channels in nerve. *J. Gen. Physiol.* 61:687–708.

Yang, J., P.T. Ellinor, W.A. Sather, J.F. Zhang, and R.W. Tsien. 1993. Molecular determinants of Ca^{2+} selectivity and ion permeation in L-type Ca^{2+} channels. *Nature.* 366:158–161.

Zhang, H., and A. Karlin. 1998. Contribution of the beta subunit M2 segment to the ion-conducting pathway of the acetylcholine receptor. *Biochemistry.* 37:7952–7964.